Anomalous Hall Effect in Type-II Weyl Semimetals

A. A. Zyuzin[1,2] and Rakesh P. Tiwari[1]

[1]*Department of Physics, University of Basel, Klingelbergstrasse 82, CH-4056 Basel, Switzerland*
[2]*A.F.Ioffe Physico-Technical Institute, 194021 St. Petersburg, Russia*

(Dated: January 11, 2016)

Recently, a new type of Weyl semimetals called type-II Weyl semimetals has been proposed. Unlike the usual (type-I) Weyl semimetals, which have a point-like Fermi surface, this new type of Weyl semimetals have a tilted conical spectrum around the Weyl point. Here we calculate the anomalous Hall conductivity of a Weyl semimetal with a tilted conical spectrum for a pair of Weyl points, using the Kubo formula. We find that the Hall conductivity is not universal and can change sign as a function of the parameters quantifying the tilts. Our results suggest that even for the case where the separation between the Weyl points vanishes, tilting of the conical spectrum could give rise to a finite anomalous Hall effect, if the tilts of the two cones are not identical.

PACS numbers: 73.43.-f, 71.90.+q, 03.65.Vf, 75.47.-m

I. INTRODUCTION

In recent years, condensed matter systems with topologically nontrivial band structures have generated a lot of interest. One particularly intriguing topological system is the three-dimensional Weyl semimetal[1]. In the simplest possible realization of a Weyl semimetal, there are at least two *distinct* points in the Brillouin zone (BZ), where the conduction and the valence bands touch. These points are called Weyl points (WPs) and they always come in pairs. Usually these WPs are protected by some crystalline symmetry and the two WPs forming a pair represent a source and a sink of Berry curvature[2–9]. Experimental realizations of WPs have been reported in TaP, NbP, TaAs, NbAs[10–16]. The topological nature of Weyl semimetals gives rise to Fermi arc surface states, the quantum anomalous Hall effect, and chiral-anomaly related negative magnetoresistance[17–24].

Most recently, a new type of Weyl semimetal, with a tilted conical spectrum, such that the WP transforms to a Dirac line or a Fermi surface has been proposed[25]. These Weyl semimetals are now called type-II Weyl semimetals (WSM2s) and WTe_2 is a possible candidate for an experimental realization of such a phase[26]. The various transport and thermodynamic properties of these WSM2 are very different from those of the usual type-I Weyl semimetal (WSM1), partially due to marked differences in the density of states of the type-I and type-II Weyl semimetals at the Fermi level. Ideal WSM1 has a conical spectrum and a point-like Fermi surface at the WP. Imagine this conical spectrum *getting* tilted towards some direction in the Brillouin zone (see Figs. 1 and 2). This tilt can be attributed to strain or chemical doping of the original WSM1. If this tilt is small enough such that the Fermi surface remains point-like, the system is still classified as WSM1. However, large tilting of the conical spectrum results in a Lifshitz transition to a new phase classified as WSM2, where the Fermi surface is no longer point-like[25,26]. Instead, now the density of states at the WP is *finite*. For a linearized model as shown in Figs. 1 and 2, the density of states at the Fermi level depends upon the cutoff Λ in momentum space, beyond which a linear description of the excitations around the WP is no longer valid. As noted in Ref. 26, it is possible to have a WSM2, where one WP is of type-I and its partner (of opposite chirality) WP is of type-II.

Due to the tilted conical spectrum, the thermodynamic and transport properties of WSM2 can be dramatically different from their counterparts in WSM1[26]. In particular, Ref. 26 points out the absence of a chiral-anomaly in WSM2, if the external magnetic field is applied along an axis perpendicular to the direction of tilt of the conical spectrum. In other words, the chiral-anomaly related negative magnetoresistance in WSM2 is anisotropic.

In this article, we investigate the anomalous Hall effect (AHE) in WSM2 and compare our results with the AHE in WSM1. The AHE in WSM1 is fully determined by the location of the WPs in BZ[27]. We find that in addition to the location of the WPs in the BZ, the AHE in WSM2 depends crucially on the tilts of the conical spectrum around the two WPs. We explore two distinct regimes, one where the tilts are in the direction pointing along the line separating the two WPs (see Fig. 1) and the other where the tilts are in a direction perpendicular to the line separating the two WPs (see Fig. 2). For each of these regimes, we consider various possible tilting angles for the two WPs.

The rest of this article is organized as follows. In the next section (Sec. II) we describe our model and the calculation of the AHE in WSM2. In Sec. III, we present a discussion of our results, highlighting the key differences between the AHE in WSM1 and WSM2, and finally in Sec. IV, we present a summary of our main results before presenting our concluding remarks.

II. AHE IN WSM2

Consider the simplest kind of Weyl semimetal state with only two WPs. To be classified as WSM2, at least one of these WPs should have a tilt in some direction in the BZ, such that the Fermi surface around that WP is

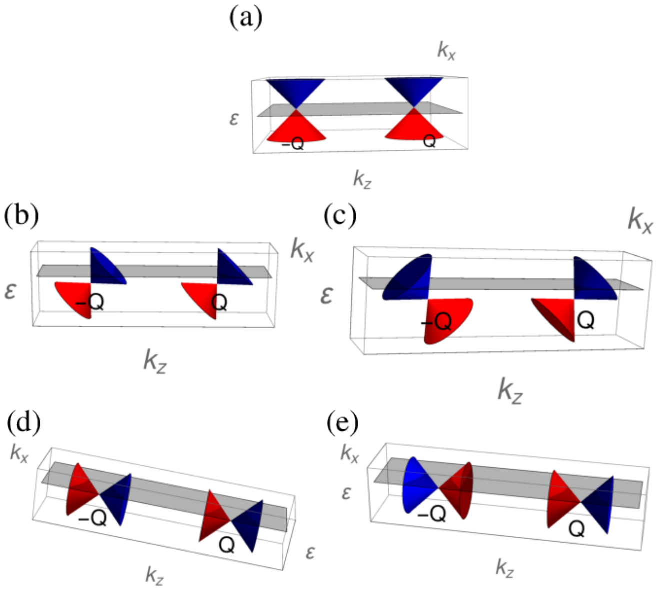

FIG. 1. (color online) The tilted conical spectrum around the Weyl points (WPs). (a) Two WPs of type-I. The WPs are located at $\pm Q\mathbf{e}_z$ and the low-energy excitations around these WPs are described by the Hamiltonians in Eq.(1), where $C_1 = C_2 = 0$. (b) Tilting the original WPs towards k_z, where the tilts for both WPs are in the same direction. The low-energy excitations around these WPs are described by the Hamiltonians in Eq.(1), where $C_1 = C_2 = v$. (c) Tilting the original WPs towards k_z, where the tilts for both WPs are in the opposite direction. The low-energy excitations around these WPs are described by the Hamiltonians in Eq.(1), where $C_1 = -C_2 = v$. (d) By increasing the tilts in (b) further, we can reach a situation, where the axis of both cones is along $\mathbf{e}_z$ (corresponding to $C_1 = C_2 \to \infty$). (e) By increasing the tilts in (c) further, we can reach a situation, where the axis of both cones is along $\pm\mathbf{e}_z$ (corresponding to $C_1 = -C_2 \to \infty$). The grey plane corresponds to the chemical potential μ, measured from the WPs, which are located at $\varepsilon = 0$. For (a) $\mu = 0$, while in (b), (c), (d), and (e) $\mu > 0$.

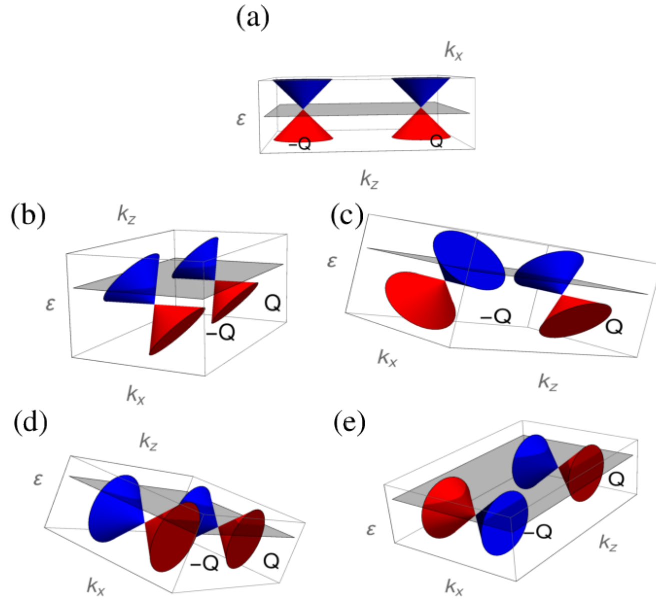

FIG. 2. (color online) The tilted conical spectrum around the Weyl points (WPs). (a) Two WPs of type-I. The WPs are located at $\pm Q\mathbf{e}_z$ and the low-energy excitations around these WPs are described by the Hamiltonians in Eq.(9), where $C_1 = C_2 = 0$. (b) Tilting the original WPs towards k_x, where the tilts for both WPs are in the same direction. The low-energy excitations around these WPs are described by the Hamiltonians in Eq.(9), where $C_1 = C_2 = v$. (c) Tilting the original WPs towards k_x, where the tilts for both WPs are in the opposite direction. The low-energy excitations around these WPs are described by the Hamiltonians in Eq.(9), where $C_1 = -C_2 = v$. (d) By increasing the tilts in (b) further, we can reach a situation, where the axis of both cones is along $\mathbf{e}_x$ (corresponding to $C_1 = C_2 \to \infty$). (e) By increasing the tilts in (c) further, we can reach a situation, where the axis of both cones is along $\pm\mathbf{e}_x$ (corresponding to $C_1 = -C_2 \to \infty$). The grey plane corresponds to the chemical potential μ, measured from the WPs, which are located at $\varepsilon = 0$. For (a) $\mu = 0$, while in (b), (c), (d), and (e) $\mu > 0$

no longer point-like. We analyze the AHE in two different regimes, the first where the direction of tilt is along the direction in which the two WPs are separated and the second where the direction of tilt is orthogonal to the direction in which the two WPs are separated. In both regimes the Hall conductivity is calculated using the Kubo formula.

A. Splitting of Weyl points along the direction of tilt

The low-energy model of two WPs of opposite chirality, at the same energy, and separated in the momentum space is described by the Hamiltonian

$$\begin{aligned} H_1(\mathbf{k}) &= \hbar C_1(k_z - Q) + \hbar v \boldsymbol{\sigma}\cdot(\mathbf{k} - Q\mathbf{e}_z), \\ H_2(\mathbf{k}) &= \hbar C_2(k_z + Q) - \hbar v \boldsymbol{\sigma}\cdot(\mathbf{k} + Q\mathbf{e}_z), \end{aligned} \tag{1}$$

where $2Q$ is the distance between the WPs in momentum space along $\mathbf{e}_z$, v is the Fermi velocity when $C_1 = C_2 = 0$, and $\boldsymbol{\sigma}$ is a vector composed of the three Pauli matrices. We set $\hbar = 1$ throughout the intermediate steps of our calculation and restore it in the final expressions. The type of the WP is defined by the parameter C_χ, $\chi \in \{1, 2\}$. WP is of so-called type-II if $|C_\chi| > v$. In this case the WP coexists with the electron and hole Fermi pockets[25,26]. The one-particle Green functions have the following form

$$\begin{aligned} G_1(\omega_n, \mathbf{k}) &= \sum_{s=\pm1} \frac{(1 - s\boldsymbol{\sigma}\cdot\mathbf{N}_{\mathbf{k}-Q\mathbf{e}_z})/2}{i\omega_n + \mu - C_1(k_z - Q) + sv|\mathbf{k} - Q\mathbf{e}_z|}, \\ G_2(\omega_n, \mathbf{k}) &= \sum_{s=\pm1} \frac{(1 + s\boldsymbol{\sigma}\cdot\mathbf{N}_{\mathbf{k}+Q\mathbf{e}_z})/2}{i\omega_n + \mu - C_2(k_z + Q) + sv|\mathbf{k} + Q\mathbf{e}_z|}, \end{aligned} \tag{2}$$

where ω_n is the fermionic Matsubara frequency, μ is the chemical potential, and $\mathbf{N_k} = \mathbf{k}/k$ is the unit vector in the direction of wave-vector $\mathbf{k}$. In what follows we assume for concreteness that $\mu \geqslant 0$.

The anomalous Hall conductivity is given by the zero frequency and zero wave-vector limit of the current-current correlation function

$$\Pi_{ij}(\Omega, \mathbf{q}) = T \sum_{\omega_n} \sum_{\chi=1,2} \int \frac{d^3k}{(2\pi)^3} J_i^{(\chi)} G_\chi(\omega_n + \Omega_m, \mathbf{k} + \mathbf{q}) \times J_j^{(\chi)} G_\chi(\omega_n, \mathbf{k}) \Big|_{i\Omega_m \to \Omega + i\delta}, \quad (3)$$

where T is the temperature (the Boltzmann constant is set to unity), as:

$$\sigma_{xy} = -\lim_{\Omega \to 0} \frac{\Pi_{xy}(\Omega, 0)}{i\Omega}. \quad (4)$$

The current operators are defined as follows

$$J_i^{(1,2)} = e\left(C_{1,2}\delta_{iz} \pm v\sigma_i\right). \quad (5)$$

Performing the summation over the fermionic frequencies and taking the zero temperature limit we obtain the anomalous Hall conductivity $\sigma_{xy} = \sigma_{xy}^{(1)} + \sigma_{xy}^{(2)}$, where

$$\sigma_{xy}^{(1,2)} = \mp \frac{e^2}{8\pi^2} \int_{-\Lambda \mp Q}^{\Lambda \mp Q} dk_z \Big\{ \mathrm{sign}(k_z)\Theta(v^2k_z^2 - (C_{1,2}k_z - \mu)^2) + \frac{vk_z}{|C_{1,2}k_z - \mu|}(1 - \Theta(v^2k_z^2 - (C_{1,2}k_z - \mu)^2)) \Big\}. \quad (6)$$

Here we have introduced a momentum cut-off Λ along the z-axis. This cut-off is necessary for correct evaluation of the AHE for Weyl semimetals within the linear dispersion model[28]. For the WSM2, the momentum cut-off Λ is a measure of the density of states due to electron and hole Fermi pockets. In the limit when the Fermi energy is at the charge neutrality point, $\mu = 0$, we find that the Hall conductivity is a non-analytic function of $C_{1,2}$:

$$\sigma_{xy} = \frac{e^2Q}{2\pi^2\hbar}\left[\min\left(1, \frac{v}{|C_1|}\right) + \min\left(1, \frac{v}{|C_2|}\right)\right]\frac{1}{2}. \quad (7)$$

Here, we have restored the Planck constant $\hbar$. Note that σ_{xy} does not depend on $C_{1,2}$ for $|C_{1,2}| < v$, while it becomes non universal at $|C_{1,2}| > v$ and decreases with an increase of $|C_1|$ or $|C_2|$. In both limits σ_{xy} is proportional to the distance between the WPs[3]. The condition $|C_\chi| = v$ describes the case when the Weyl cone touches the Fermi level. Thus the non analytic behaviour of the anomalous Hall conductivity is related to the van-Hove singularity in the density of states at the Fermi level.

The dependence of the Hall conductivity on $C_{1,2}$ at a finite chemical potential is shown in Fig. 3 . We observe that the Hall conductivity has a peak or a dip at $|C_{1,2}| = v$ depending on the sign of $C_{1,2}$. The height of the peak or dip diverges logarithmically with the cut-off Λ as

$$\sigma_{xy} = \frac{e^2}{2\pi^2\hbar}\left[Q + \frac{\mu}{4\hbar}\left(\frac{1}{C_2} - \frac{1}{C_1}\right)\left(\ln\left|\frac{2\hbar v\Lambda}{\mu}\right| - 1\right)\right]. \quad (8)$$

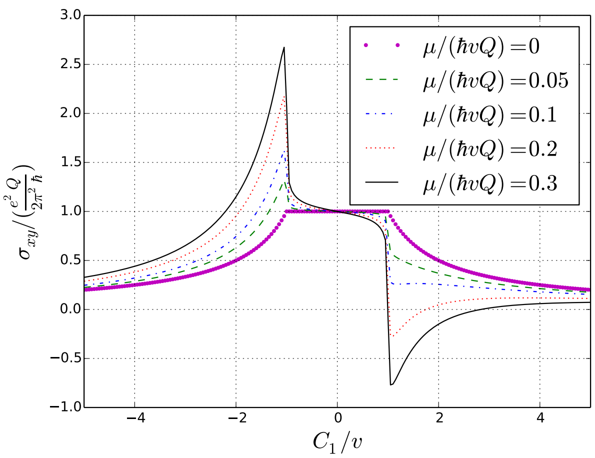

FIG. 3. (color online) Normalized anomalous Hall conductivity $\sigma_{xy}/(\frac{e^2Q}{2\pi^2\hbar})$ as a function of the parameter C_1/v for different values of the normalized chemical potential $\mu/(\hbar vQ)$, and fixed $C_2 = -C_1$. Fig. 1(c) and Fig. 1(e) show the spectrum for this situation corresponding to $C_1 = v$ and $C_1 = \infty$ respectively.

Thus, there is a peak in the Hall conductivity when $C_2 = v$ and $C_1 = -v$ and a dip when $C_2 = -v$ and $C_1 = v$. Interestingly, σ_{xy} is finite at $\mu > 0$ even if the separation between WPs vanishes, $Q = 0$. This observation implies that for a finite μ even a Dirac semimetal ($Q = 0$) with a tilted conical spectrum such that $C_1 \neq C_2$, will show a finite AHE. It is the contribution from the states at the Fermi surface which gives rise to a finite value of anomalous Hall conductivity at $\mu > 0$. We find that the anomalous Hall conductivity diverges logarithmically with the cutoff. This divergence arises due to the presence of unbounded electron - hole pockets at the Fermi surface, for $|C_\chi| \geq v$.

B. Splitting of Weyl points orthogonal to the direction of tilt

The low-energy model of two WPs in the case when the direction of tilt is orthogonal to the splitting of the WPs is described by the Hamiltonians

$$H_1(\mathbf{k}) = \hbar C_1 k_x + \hbar v \boldsymbol{\sigma} \cdot (\mathbf{k} - Q\mathbf{e}_z)$$
$$H_2(\mathbf{k}) = \hbar C_2 k_x - \hbar v \boldsymbol{\sigma} \cdot (\mathbf{k} + Q\mathbf{e}_z) \quad (9)$$

A calculation similar to the one performed in the previous section gives $\sigma_{xy} = \sigma_{xy}^{(1)} + \sigma_{xy}^{(2)}$, where

$$\sigma_{xy}^{(1,2)} = \pm \frac{e^2}{16\pi^3} \int_{-\Lambda \mp Q}^{\Lambda \mp Q} dk_z k_z \int_{-\infty}^{\infty} \frac{dk_x dk_y}{k^3} \times \Big[\Theta\Big(\mu - C_{1,2}k_x - vk\Big) - \Theta\Big(\mu - C_{1,2}k_x + vk\Big)\Big]. \quad (10)$$

In the limit $\Lambda \gg \mu$ we recover the expression in Eq.(7), which is independent on the Fermi energy. Thus, in the case $|C_\chi| < v$ the anomalous Hall conductivity does not depend on the parameters C_χ and is given by the $\sigma_{xy} = \frac{e^2 Q}{2\pi^2\hbar}$, while in the case $|C_\chi| > v$ the conductivity is not universal and decays with an increase of $|C_\chi|$. Interestingly, the integral in Eq. (10) vanishes if $Q = 0$ even at finite values of the Fermi energy, resulting in a vanishing AHE, which is in contrast to the case when the Weyl cones are tilted along the z-axis. Tilting the Weyl cone in the x-direction does not break either time reversal or inversion along the z-direction symmetries, thus we get no additional contribution in the σ_{xy}.

III. DISCUSSION

Our results indicate that the AHE in WSM2 depends crucially on the parameters C_1 and C_2, and can be used to measure these parameters. The total Hall conductivity of the Weyl semimetal is a sum of the Hall conductivity due to both WPs ($\sigma_{xy} = \sigma_{xy}^{(1)} + \sigma_{xy}^{(2)}$). First we discuss the case, where the tilt is in $\mathbf{e}_z$. If both WPs are of type-I, ($|C_1| < v$ and $|C_2| < v$) the Hall conductivity for $\mu = 0$ is universal (independent of the parameters C_1 and C_2) and is given by $\sigma_{xy} = \frac{e^2 Q}{2\pi^2\hbar}$. If one of the WPs is of type-I and the other of type-II, for e.g., $|C_1| > v$ and $|C_2| < v$, the total Hall conductivity for $\mu = 0$ is independent of C_2 but depends upon C_1, and is given by $\sigma_{xy} = \frac{e^2 Q}{4\pi^2\hbar}(1 + \frac{v}{|C_1|})$. The *decreasing* contribution from the WP of type-II can be understood as follows. Due to the tilting of the conical spectrum of the WP of type-II the Hall conductivity now has a contribution from both electron and hole like carriers. In fact the contribution of this type-II WP vanishes completely in the limit $|C_1| \to \infty$ and the total Hall conductivity becomes $\sigma_{xy} = \frac{e^2 Q}{4\pi^2\hbar}$. If both WPs are of type-II, the Hall conductivity in general depends upon both parameters $|C_1| > v$ and $|C_2| > v$. A particularly interesting situation is reached if the tilts of the two WPs are opposite to each other. Fig. 3 shows the anomalous Hall conductivity in this situation for various values of μ and $C_2 = -C_1$. Note that when we have a WSM2, the Hall conductivity changes sign as a function of C_1 (in the right half $C_1 > v$) for large values of μ. The decreasing contribution from the WP of type-II is also observed when the tilt is in $\mathbf{e}_x$ [see Eq.(10)].

It is important to stress that our calculations are performed using a linear dispersion model of the excitations around the WPs. An unbounded linear dispersion is not realistic for a solid state realization of WSM2. In a realistic case the linear dispersion will have a cut-off (Λ) in momentum space, beyond which the excitations in WSM2 are no longer described by a linearized model. This cut-off Λ is also a measure of the density of states at the WP for a WSM2. The contribution of these large momentum ($> \Lambda$) states is ignored in our calculation. Another crucial point to note is that the conduction and the valence bands for the two distinct WPs are connected in the BZ by these large momentum states. Figs. 1 and 2 suggest that the electronic band-structure of the WSM2 can be drastically modified for large values of the parameters C_1 and C_2. Thus, in general the contribution of the large momentum states to the AHE will depend upon the details of the electronic band-structure of a specific realization of WSM2 and will not be universal.

Finally, we estimate the value of the anomalous Hall conductivity considering WTe_2 as a possible WSM2. Assuming the splitting between the two WPs to be $Q = (0.01)\text{Å}^{-1}$, we obtain $\sigma_{xy} = \frac{e^2 Q}{2\pi^2\hbar} \approx 10$ per Ohm per cm, which is of the same order as the anomalous Hall conductivity in magnetic conductors[29]. The dependence of $\sigma_{xy}/(\frac{e^2 Q}{2\pi^2\hbar})$ on the Fermi energy is shown in Fig.3.

IV. SUMMARY

We have investigated the anomalous Hall effect in type-II Weyl semimetal within a linear dispersion model using the Kubo formula. Our findings suggest that unlike in type-I Weyl semimetal, the anomalous Hall effect in type-II Weyl semimetal is not universal and in general depends on the parameters quantifying the tilt of the conical spectrum around the Weyl points. So far there has been no experimental evidence for the existence of type-II Weyl semimetal. Thus, a measurement of the anomalous Hall effect can help in categorizing the two different types of Weyl semimetals. If the Weyl semimetal is of type-II, the measurement of anomalous Hall effect can provide information about the tilt parameters associated with these type-II Weyl semimetals. By applying strain and thereby changing the lattice constant for materials such as HgTe[30], one can potentially measure the anomalous Hall effect as a function of the tilt parameters and verify our predictions.

ACKNOWLEDGMENTS

We would like to acknowledge fruitful discussions with A. Burkov and C. Bruder. The work was financially supported by the Swiss SNF and the NCCR Quantum Science and Technology.

[1] S. Murakami, New Journal of Physics **9**, 356 (2007).
[2] X. Wan, A. M. Turner, A. Vishwanath, and S. Y. Savrasov, Phys. Rev. B **83**, 205101 (2011).
[3] A. A. Burkov and L. Balents, Phys. Rev. Lett. **107**, 127205 (2011).

[4] A. A. Burkov, M. D. Hook, and L. Balents, Phys. Rev. B **84**, 235126 (2011).
[5] G. B. Halász and L. Balents, Phys. Rev. B **85**, 035103 (2012).
[6] A. A. Zyuzin, S. Wu, and A. A. Burkov, Phys. Rev. B **85**, 165110 (2012).
[7] C.-X. Liu, P. Ye, and X.-L. Qi, Phys. Rev. B **87**, 235306 (2013).
[8] K.-Y. Yang, Y.-M. Lu, and Y. Ran, Phys. Rev. B **84**, 075129 (2011).
[9] G. E. Volovik, *The Universe in a Helium Droplet* (Clarendon Press; Oxford University Press, 2009).
[10] S.-Y. Xu, I. Belopolski, N. Alidoust, M. Neupane, G. Bian, C. Zhang, R. Sankar, G. Chang, Z. Yuan, C.-C. Lee, S.-M. Huang, H. Zheng, J. Ma, D. S. Sanchez, B. Wang, A. Bansil, F. Chou, P. P. Shibayev, H. Lin, S. Jia, and M. Z. Hasan, Science **349**, 613 (2015).
[11] B. Lv, N. Xu, H. Weng, J. Ma, P. Richard, X. Huang, L. Zhao, G. Chen, C. Matt, F. Bisti, V. Strocov, J. Mesot, Z. Fang, X. Dai, T. Qian, M. Shi, and H. Ding, Nature Physics **11**, 724 (2015).
[12] B. Q. Lv, H. M. Weng, B. B. Fu, X. P. Wang, H. Miao, J. Ma, P. Richard, X. C. Huang, L. X. Zhao, G. F. Chen, Z. Fang, X. Dai, T. Qian, and H. Ding, Phys. Rev. X **5**, 031013 (2015).
[13] C. Shekhar, A. K. Nayak, Y. Sun, M. Schmidt, M. Nicklas, I. Leermakers, U. Zeitler, Y. Skourski, J. Wosnitza, Z. Liu, Y. Chen, W. Schnelle, H. Borrmann, Y. Grin, C. Felser, and B. Yan, Nature Physics **11**, 645 (2015).
[14] L. X. Yang, Z. K. Liu, Y. Sun, H. Peng, H. F. Yang, T. Zhang, B. Zhou, Y. Zhang, Y. F. Guo, M. Rahn, D. Prabhakaran, Z. Hussain, S.-K. Mo, C. Felser, B. Yan, and Y. L. Chen, Nature Physics **11**, 728 (2015).
[15] S.-Y. Xu, N. Alidoust, I. Belopolski, Z. Yuan, G. Bian, T.-R. Chang, H. Zheng, V. N. Strocov, D. S. Sanchez, G. Chang, C. Zhang, D. Mou, Y. Wu, L. Huang, C.-C. Lee, S.-M. Huang, B. Wang, A. Bansil, H.-T. Jeng, T. Neupert, A. Kaminski, H. Lin, S. Jia, and M. Zahid Hasan, Nature Physics **11**, 748 (2015).
[16] C. Zhang, Z. Yuan, S. Xu, Z. Lin, B. Tong, M. Zahid Hasan, J. Wang, C. Zhang, and S. Jia, ArXiv e-prints (2015), arXiv:1502.00251 [cond-mat.mtrl-sci].
[17] H. Nielsen and M. Ninomiya, Physics Letters B **130**, 389 (1983).
[18] A. A. Zyuzin and A. A. Burkov, Phys. Rev. B **86**, 115133 (2012).
[19] P. Hosur and X. Qi, Comptes Rendus Physique **14**, 857 (2013).
[20] A. A. Burkov, Journal of Physics: Condensed Matter **27**, 113201 (2015).
[21] D. T. Son and B. Z. Spivak, Phys. Rev. B **88**, 104412 (2013).
[22] C. Zhang, S.-Y. Xu, I. Belopolski, Z. Yuan, Z. Lin, B. Tong, N. Alidoust, C.-C. Lee, S.-M. Huang, H. Lin, M. Neupane, D. S. Sanchez, H. Zheng, G. Bian, J. Wang, C. Zhang, T. Neupert, M. Zahid Hasan, and S. Jia, ArXiv e-prints (2015), arXiv:1503.02630 [cond-mat.mes-hall].
[23] J. Xiong, S. K. Kushwaha, T. Liang, J. W. Krizan, W. Wang, R. J. Cava, and N. P. Ong, ArXiv e-prints (2015), arXiv:1503.08179 [cond-mat.str-el].
[24] X. Huang, L. Zhao, Y. Long, P. Wang, D. Chen, Z. Yang, H. Liang, M. Xue, H. Weng, Z. Fang, X. Dai, and G. Chen, Phys. Rev. X **5**, 031023 (2015).
[25] G. Volovik and M. Zubkov, Nuclear Physics B **881**, 514 (2014).
[26] A. A. Soluyanov, D. Gresch, Z. Wang, Q. Wu, M. Troyer, X. Dai, and B. A. Bernevig, Nature **527**, 495 (2015).
[27] A. A. Burkov, Phys. Rev. Lett. **113**, 187202 (2014).
[28] P. Goswami and S. Tewari, Phys. Rev. B **88**, 245107 (2013).
[29] S. Nakatsuji, N. Kiyohara, and T. Higo, Nature **527**, 212 (2015).
[30] J. Ruan, S.-K. Jian, H. Yao, H. Zhang, S.-C. Zhang, and D. Xing, ArXiv e-prints (2015), arXiv:1511.08284 [cond-mat.mes-hall].